Highly Efficient Light-Harvesting System Based on a Phosphorescent Acceptor Coupled with Dendrimer Donors via Singlet−Singlet and Triplet−Triplet Energy Transfer

Tae-Hyuk Kwon,[†] Myoung Ki Kim,[†] Jongchul Kwon,[†] Dae-Yup Shin,[‡] Su Jin Park,[‡] Chang-Lyoul Lee,[§,||] Jang-Joo Kim,[§] and Jong-In Hong*[,†]

Department of Chemistry, College of Natural Sciences, and School of Materials Sciences and Engineering, Center for Organic Light Emitting Diodes, Seoul National University, Seoul 151-747, Korea, and Corporate Research and Development Center, Samsung SDI, Yongin 449-902, Korea

Received February 27, 2007. Revised Manuscript Received April 19, 2007

A series of efficient light-harvesting systems (FIr3mG*x*, $x = 1-3$) based on dendrimer donor (mCP: *N*,*N*′-dicarbazolyl-3,5-benzene) derivatives coupled with a sky blue phosphorescent acceptor (FIrpic: iridium(III) bis[(4,6-difluorophenyl)pyridinato-*N*,$C^{2'}$]-3-hydroxypicolinate derivative) were prepared, and their photophysical properties were investigated. The light-harvesting ability of FIr3mG*x* ($x = 1-3$) increases with the number of energy donor mCP units. The acceptor PL intensity of the donor−acceptor conjugate dendrimers (FIr3mG*x*, $x = 1-3$) increases over 6 times with the number of mCP units via sensitization from the light-harvesting antenna after excitation at the donor absorption ($\lambda_{ex} = 310$ nm), as compared to that of only an acceptor without a donor (FIrpic) upon excitation at the MLCT region ($\lambda_{ex} = 380$ nm) because of efficient intramolecular singlet−singlet and triplet−triplet energy transfer from the donor to the acceptor and less luminance quenching induced by the bulky dendrimer structure. The singlet−singlet intramolecular energy transfer in FIr3mG*x* from the dendrimer donor to the acceptor exhibits a high efficiency of greater than 90% via the steady-state PL method and 94% via the transient PL method. Additionally, the triplet−triplet energy transfer efficiency via the transient PL method exhibits an efficiency greater than 99%. This indicates that FIr3mG*x* exhibits good light-harvesting abilities because the mCP unit is an efficient light absorber and because the core FIrpic functions as a spatial energy concentrator that drains energy from the dendrimer donor.

Introduction

Dendrimer materials are promising candidates for various applications such as organic light-emitting diodes (OLEDs) for spin-coatable full color displays and as light-harvesting systems that transform natural solar energy into chemical energy. Phosphorescent dendrimer materials for OLEDs have recently attracted considerable attention because they possess the advantages of both small molecules[1,2] and polymer materials,[3] such as high efficiency, easy accessibility and solution processing, and control over intermolecular interactions.[4,5] However, the dendrons (peripheral moieties) in the phosphorescent dendrimers developed thus far have been employed for the purpose of preventing self-aggregation[4] or for providing charge transporting properties.[5] Thus, multifunctional dendrons with not only the aforementioned properties but also an energy donor ability are expected to improve the efficiency of devices comprising dendrimer OLEDs. Furthermore, dendrimer structures have been used in light-harvesting systems because the energy donor moiety and the acceptor unit can be easily attached at the peripheral and core sites, respectively.[6−12] However, most of the light-

* Corresponding author. E-mail: jihong@snu.ac.kr.
[†] College of Natural Sciences, Seoul National University.
[‡] Samsung SDI.
[§] Center for Organic Light Emitting Diodes, Seoul National University.
[||] Current address: Cavendish Laboratory, University of Cambridge, Madingley Rd., Cambridge CB3 0HE, U.K.

(1) (a) Baldo, M. A.; O'Brien, D. F.; You, Y.; Shoustikov, A.; Sibly, S.; Thompson, M. E.; Forrest, S. R. *Nature* **1998**, *395*, 151. (b) Adachi, C.; Baldo, M. A.; Thompson, M. E.; Forrest, S. R. *J. Appl. Phys.* **2001**, *90*, 5048.
(2) Holmes, R. J.; Forrest, S. R.; Tung, Y.-J.; Kwong, R. C.; Brown, J. J.; Garon, S.; Thompson, M. E. *Appl. Phys. Lett.* **2003**, *82*, 2422.
(3) Friend, R. H.; Gymer, R. W.; Holmes, A. B.; Burroughes, J. H.; Marks, R. N.; Taliani, C.; Bradley, D. D. C.; Dos Santos, D. A.; Bredas, J. L.; Lögdlund, M.; Salaneck, W. R. *Nature* **1999**, *397*, 121.
(4) (a) Lo, S.-C.; Male, N. A. H.; Markham, J. P. J.; Magennis, S. W.; Burn, P. L.; Salata, O. V.; Samuel, I. D. W. *Adv. Mater.* **2002**, *14*, 975. (b) Markham, J. P. J.; Lo, S.-C.; Magennis, S. W.; Burn, P. L.; Samuel, I. D. W. *Appl. Phys. Lett.* **2002**, *80*, 2645. (c) Anthopoulos, T. D.; Markham, J. P. J.; Namdas, E. B.; Samuel, I. D. W.; Lo, S.-C.; Burn, P. L. *Appl. Phys. Lett.* **2003**, *82*, 4824. (d) Lo, S.-C.; Anthopoulos, T. D.; Namdas, E. B.; Burn, P. L.; Samuel, I. D. W. *Adv. Mater.* **2005**, *17*, 1945. (e) Anthopoulos, T. D.; Frampton, M. J.; Namdas, E. B.; Burn, P. L.; Samuel, I. D. W. *Adv. Mater.* **2004**, *16*, 557. (f) Lo, S.-C.; Richards, G. J.; Markham, J. P. J.; Namdas, E. B.; Sharma, S.; Burn, P. L.; Samuel, I. D. W. *Adv. Funct. Mater.* **2005**, *15*, 1451.
(5) (a) Tsuzuki, T.; Shirasawa, N.; Suzuki, T.; Tokito, S. *Jpn. J. Appl. Phys., Part 1* **2005**, *44* (6A), 4151. (b) Ding, J.; Cao, J.; Cheng, Y.; Xie, Z.; Wang, L.; Ma, D.; Jing, X.; Wang, F. *Adv. Funct. Mater.* **2006**, *16*, 575.
(6) Neuwahl, F. V. R.; Righini, R.; Adronov, A.; Malenfant, P. R. L.; Fréchet, J. M. J. *J. Phys. Chem. B* **2001**, *105*, 1307.
(7) (a) Jiang, D.-L.; Aida, T. *Nature* **1997**, *388*, 454. (b) Aida, T.; Jiang, D.-L.; Yashima, E.; Okamoto, Y. *Thin Solid Films* **1998**, *331*, 254.
(8) Kawa, M.; Fréchet, J. M. J. *Chem. Mater.* **1998**, *10*, 286.
(9) (a) Gilat, S. L.; Adronov, A.; Fréchet, J. M. J. *Angew. Chem., Int. Ed.* **1999**, *38*, 1422; Ibid. *Angew. Chem., Int. Ed.* **1999**, *111*, 1519. (b) Adronov, A.; Gilat, S. L.; Fréchet, J. M. J.; Ohta, K.; Neuwahl, F. V. R.; Fleming, G. R. *J. Am. Chem. Soc.* **2000**, *122*, 1175.
(10) Thomas, K. R. J.; Thompson, A. L.; Sivakumar, A. V.; Bardeen, C. J.; Thayumanavan, S. *J. Am. Chem. Soc.* **2005**, *127*, 373.

10.1021/cm070536k CCC: $37.00
Published on Web 06/20/2007

Scheme 1. Synthesis of Dendrimer Donor Precursor Molecules

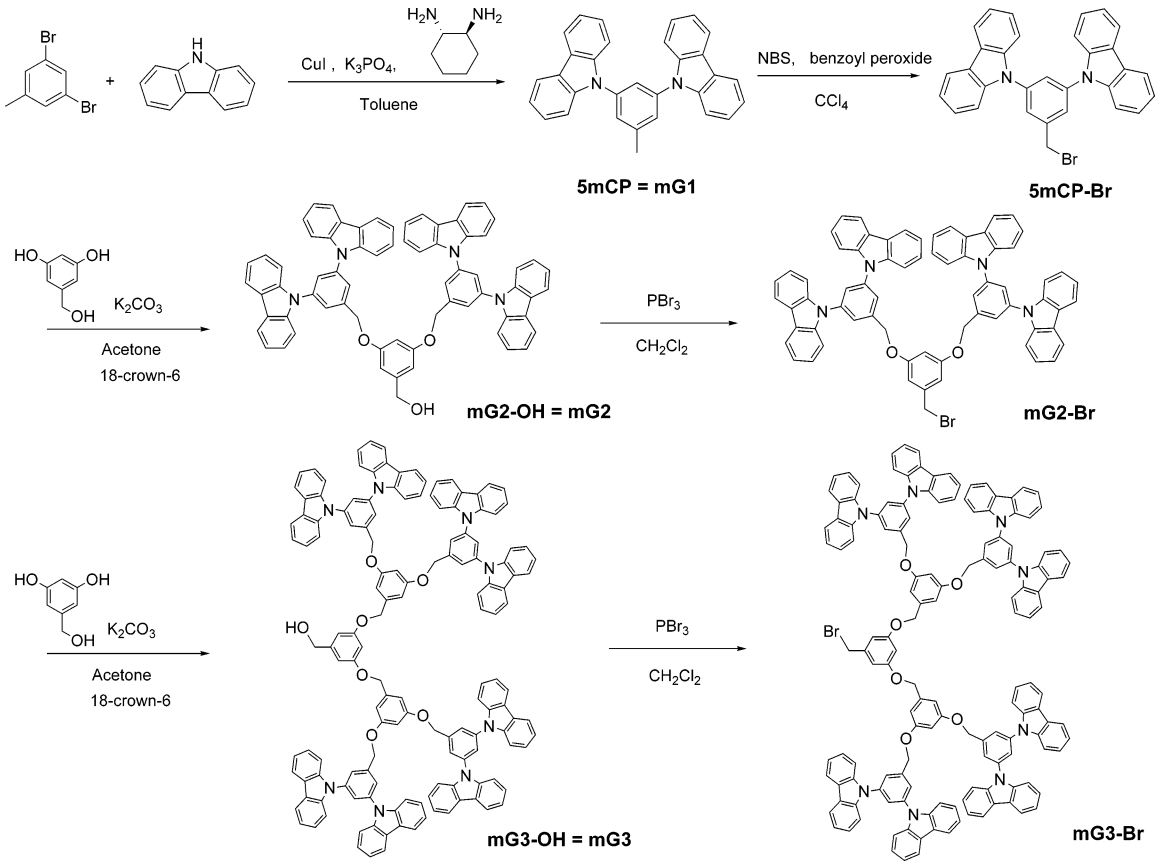

harvesting dendrimers utilize an intramolecular singlet−singlet (S−S) energy transfer (ET) mechanism.[6−10] Further, there are few reports on employing dendrimers for light harvesting through the triplet−triplet (T−T) ET mechanism,[11,12] although it is more efficient than the S−S ET mechanism in electronic devices.[1,2]

In this paper, we report a new phosphorescent dendrimer system in which a phosphorescent acceptor at the core site is covalently attached to a dendrimer donor at the peripheral site via a nonconjugated bridge. The donor (mCP: *N*,*N*′-dicarbazolyl-3,5-benzene) derivatives were coupled with the acceptor (FIrpic: iridium(III) bis[(4,6-difluorophenyl)pyridinato-*N*,*C*$^{2'}$]-picolinate derivative) by a nonconjugated benzyl ether linker. The benzyl ether linker was introduced to isolate the photophysical properties of both the donor (mCP) and the acceptor. Moreover, these donor−acceptor conjugates are fairly different from the known dendrimer OLED emitting layer materials.[4,5] This is because, in this case, the peripheral moieties not only prevent self-aggregation but also donate energy to the core. Therefore, this system provides improved efficiency through intramolecular ET in addition to the advantages of a typical dendrimer. Furthermore, this system reports on a dendrimer light-harvesting system that simultaneously uses both the S−S and the T−T ET mechanisms and therefore results in an increase in the acceptor emission intensity. Herein, we present the synthesis of dendrimer donor−acceptor conjugates and their photophysical properties.

Results and Discussion

Synthesis. Dendrimer donor precursor molecules (mG1-Br, mG2-Br, and mG3-Br) were prepared by a convergent method (Scheme 1).[13] An mCP derivative (5mCP = 5-methyl-*N*,*N*′-dicarbazolyl-1,3-benzene = mG1) was prepared according to the Buchwald procedure.[22] mG1 was then converted to the corresponding bromomethyl compound (5mCP-Br) in 56% yield, upon treatment with NBS/benzoyl peroxide, and then 5mCP-Br was coupled with 3,5-dihydroxybenzyl alcohol in acetone to produce mG2-OH in 85% yield. mG2-OH was treated with PBr_3 in methylene chloride to give rise to mG2-Br in 92% yield after purification by column chromatography. mG3-OH and mG3-Br were prepared through the previous synthetic steps iteratively. Cyclometalated Ir(III) μ-chloro-bridged dimers of the general formula $C\hat{}N_2Ir(\mu\text{-}Cl)_2IrC\hat{}N_2$ were synthesized by refluxing $IrCl_3 \cdot nH_2O$ with a cyclometalating ligand in a 3:1 mixture of 2-methoxyethanol and water. A mixture of the chloro-bridged dimer, 3-hydroxypicolinic acid, and sodium carbonate was refluxed in an inert atmosphere in 2-ethoxyethanol to provide FIrpicOH. FIrpicOH was subsequently coupled with donor molecules (mG*x*-Br) to produce the corresponding

(11) (a) Bergamini, G.; Saudan, C.; Ceroni, P.; Maestri, M.; Balzani, V.; Gorka, M.; Lee, S.-K.; Heyst, J. V.; Vögtle, F. *J. Am. Chem. Soc.* **2004**, *126*, 16466. (b) Chen, J.; Chen, J.; Li, S.; Zhang, L.; Yang, G.; Li, Y. *J. Phys. Chem. B* **2006**, *110*, 4663. (c) Zhang, L.; Chen, J.; Li, S.; Chen, J.; Li, Y.-Y.; Yang, G.; Li, Y. *J. Photochem. Photobiol., A* **2006**, *181*, 429.

(12) (a) Chen, J.; Li, S.; Zhang, L.; Liu, B.; Han, Y.; Yang, G.; Li, Y. *J. Am. Chem. Soc.* **2005**, *127*, 2165. (b) Chen, J.; Chen, J.; Li, S.; Zhang, L.; Yang, G.; Li, Y. *J. Phys. Chem. B* **2006**, *110*, 4663.

(13) Hawker, C. J.; Fréchet, J. M. J. *J. Am. Chem. Soc.* **1990**, *112*, 7638.

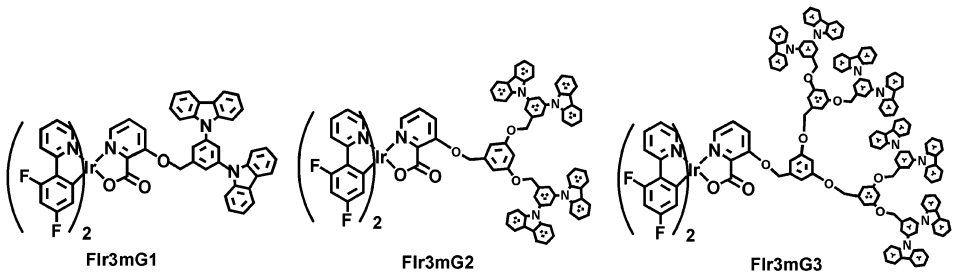

Figure 1. Molecular structures of FIr3mG1, FIr3mG2, and FIr3mG3.

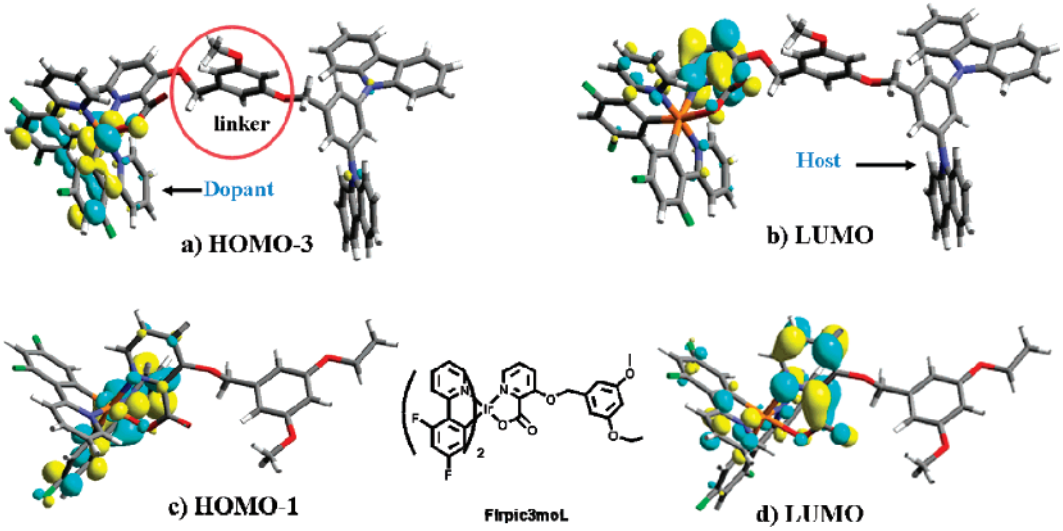

Figure 2. DFT calculations of a FIr3mG2′ unit (a) HOMO − 3 and (b) LUMO and those of a FIrpic3moL unit (c) HOMO − 1 and (d) LUMO.

Scheme 2. Synthesis of Donor−Acceptor Conjugate Molecules

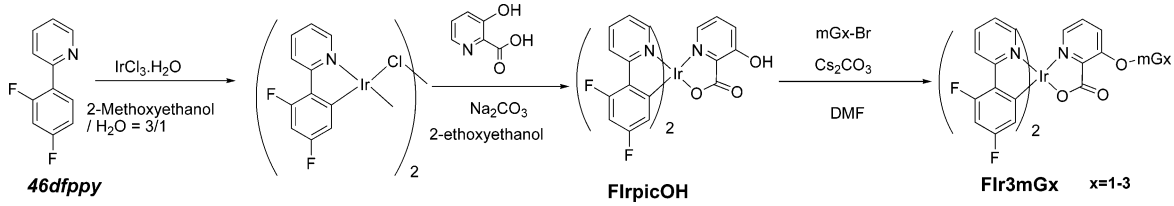

donor−acceptor conjugates—FIr3mG1, FIr3mG2, and FIr3mG3, respectively (Scheme 2 and Figure 1). Because of a large difference in R_f values in thin layer chromatography between free donors (mG*x*, $R_f = 0.6$ in CH_2Cl_2) and FIr3mG*x* ($R_f =$ 0.05 in CH_2Cl_2), there is little possibility for the existence of residual free donors in the final products after column chromatographic purification. Further, to remove any residual impurities, trituration was carried out several times in CH_2Cl_2 and hexane after column chromatography.

DFT Calculations. The density functional theory (DFT) calculations of FIr3mG2′ with only one mCP (another mCP was removed from FIr3mG2) and FIrpic3moL (acceptor analogue) were performed using the B3LYP functional with the 6-31G(*) basis set for H, C, N, and O and the Stuttgart effective core potential (ECP) for Ir (Figure 2). The low-lying triplet and singlet excited states were evaluated by time-dependent DFT (TD−-DFT) calculations. The result indicates that the T_1 transition of FIr3mG2′ corresponds to the excitation from d(Ir) + π(46dfppy) to the π(pic)* orbitals of the FIrpic3moL moiety. The T_1 emission wavelengths are 451 and 452 nm for FIr3mG2′ and FIrpic3moL, respectively. The contour plots of the molecular orbitals of FIr3mG2′ and FIrpic3moL are shown in Figure 2.[14] The T_1 transition of FIr3mG2′ is from HOMO − 3 to LUMO, where HOMO − 3 is located in phenylpyridine and LUMO in picolinic acid. This implies that the energy levels of the donor and acceptor molecules are different and do not produce a new conjugate energy level in the donor−acceptor conjugate system. In the optimized geometric structure of FIr3mG2′, the distance between the donor and the acceptor is approximately 15 Å under the assumption that all the bonds are linked through a trans geometry. Therefore, these theoretical calculations suggest that an effective triplet−triplet energy transfer between donor and acceptor takes place by the Dexter mechanism.[3]

Photophysical Properties. Figure 3a shows the absorption spectra of 5mCP (= mG1), FIrpic, FIr3mG1, FIr3mG2, and FIr3mG3. The absorbances of FIr3mG1, FIr3mG2, and FIr3mG3 in the range of 250−350 nm are very similar to those of 5mCP and increase with the number of 5mCP units. This indicates that the amount of light absorbed by the dendritic antenna doubles from one generation to the next.

(14) See the Supporting Information.

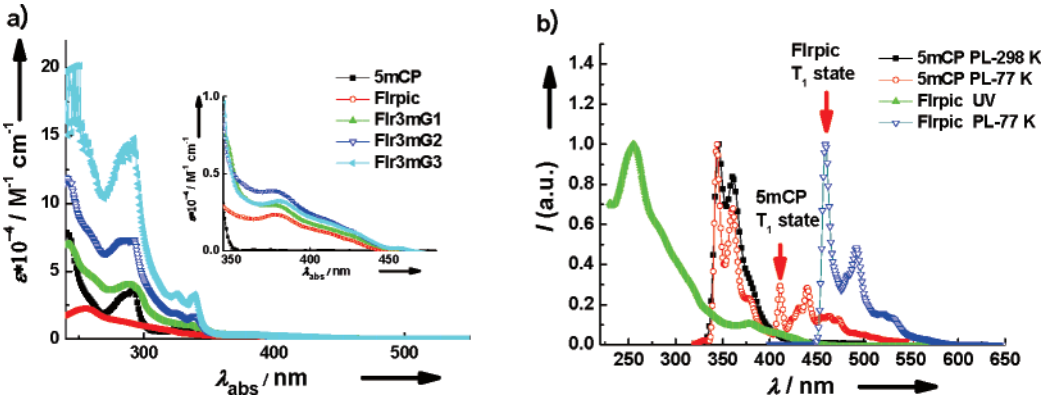

Figure 3. (a) UV spectra of 5mCP, FIrpic, and FIr3mG*x*, $x = 1-3$ in 0.02 mM 2-methyltetrahydrofuran (2-MeTHF) at 298 K. The inset shows the magnified MLCT region of FIrpic. (b) UV spectra of FIrpic and PL spectra of 5mCP and FIrpic in 0.02 mM 2-MeTHF at 298 and 77 K.

Table 1. Photophysical Properties of FIr3mG*x* and FIrpic

	emission λ_{max} (nm)[a]/ relative intensity[b]			τ (μs)			
	298 K	77 K	film	298 K[c]	77 K[d]	T_g (°C)	T_d (°C)
FIrpic	470/1	459	473/1	1.1	2.9, 2.5[e]		
FIr3mG1	470/3.1	460	475/1.5	1.1	3.1, 3.0[e]	180	299
FIr3mG2	469/4.0	459	477/3.2	1.1		175	384
FIr3mG3	470/6.3	460	475/6.6	1.1		184	396

[a] Measured in 4 μM 2-MeTHF solution. [b] Integrated acceptor emission area of the conjugate system was divided by the integrated FIrpic emission area in the range of 410−610 nm. [c] Lifetime (470 nm) upon excitation at 310 nm in 0.2 mM 2-MeTHF solution. [d] Lifetime (470 nm) upon excitation at 310 nm in 0.02 mM 2-MeTHF solution. [e] Lifetime (470 nm) in 0.2 mM 2-MeTHF solution at 77 K. The lifetime of FIrpic was measured from the excitation at 380 nm.

Further, it should be noted that there is no spectral broadening or spectral shift with increasing generations. The absorbance over 350 nm is very similar to that of FIrpic and shows little change with the number of the generation (Figure 3a, inset). This indicates that efficient light harvesting (accumulation of energy) occurs at the donor molecule (mCP unit).[14] As expected from the calculation, this result also indicates that there is no direct electronic communication between the donor and the acceptor. Figure 3b indicates a good overlap between the emission spectrum of 5mCP and the absorption spectrum of FIrpic over 350 nm (^{1}MLCT and ^{3}LC region), which ensures the S−S ET from 5mCP to FIrpic. The T−T ET from 5mCP to FIrpic can also occur because the triplet energy of 5mCP is higher than that of FIrpic.[2] Therefore, the donor−acceptor conjugate system is expected to exhibit a good ET from the donor to the acceptor via both the S−S and the T−T ET mechanisms.

The lifetime of FIr3mG*x* (470 nm) is similar to that of FIrpic: this implies an exothermic energy transfer from the donor to the acceptor (Table 1). The lifetime of FIrpic reduces with an increase in the concentration, while that of FIr3mG*x* is independent of the solution concentration. This indicates that FIr3mG*x* may be affected to a lesser extent by intermolecular quenching. Glass transition temperature (T_g) values for FIr3mG1, FIr3mG2, and FIr3mG3 were 180, 175, and 184 °C, respectively, measured by DSC, and decomposition temperature (T_d) values for FIr3mG1, FIr3mG2, and FIr3mG3 were 299, 384, and 396 °C, respectively, which correspond to a 5% weight loss in thermogravimetric analysis (TGA) under N_2 stream with scanning rate of 10 °C/min

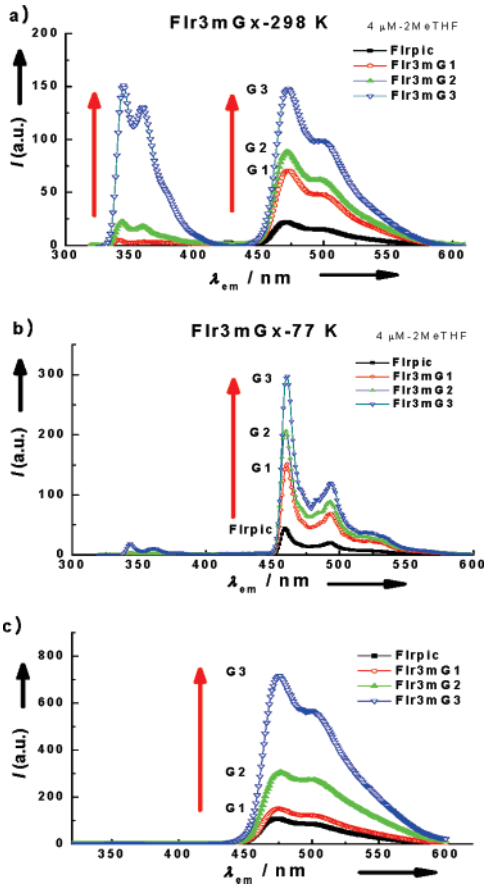

Figure 4. PL spectra (excited at 310 nm) of 4 μM FIr3mG*x* in 2-MeTHF at (a) 298 K and (b) 77 K and (c) those of the PMMA film. Each PMMA film prepared by spin-casting on quartz substrates had the same molar ratio of each phosphor (2.9 μmol).

(Table 1). These results suggest good thermal stability in FIr3mG*x*.

As shown in Table 1, the PL emission wavelengths of FIr3mG*x* are the same as that of FIrpic. This result is in good correlation with that of the DFT calculation. The PL intensity increases by over 6 times with the number of mCP units via sensitization from the light-harvesting antenna after the excitation at donor absorption (310 nm) (Figure 4). However, there is little increase in the emission intensity upon excitation at the MLCT region (380 nm) of FIr3mG*x*, as compared to the PL intensity of FIrpic (data not shown here). Therefore, PL intensity enhancement would result from

the S−S and T−T intramolecular ET from the dendrimer donor to the acceptor.

However, as shown in Figure 4a, the PL (excited at the donor absorption peak of 310 nm) intensity of the donor singlet state also increases with the generation, while that of the acceptor peak increases (G1 to G3). This may be due to the bottleneck phenomenon that prevents the further transfer of excitation from other excited states.[6,17] Or, it may be derived from the conformational heterogeneity of the dendrimers (FIr3mG*x*) that prevent energy transfer.[10] Of course, one can expect that the residual peaks are derived from the free donor impurities. However, this possibility can be ruled out. As previously mentioned in Synthesis, the final products (FIr3mG*x*) have little possibility of having residual donors due to a large difference in R_f values ($\Delta R_f = 0.55$ in CH_2Cl_2) between free donors (mG*x*) and FIr3mG*x*. Further, the residual donor peaks at 77 K show an obviously different trend from those at 298 K. For example, the residual donor peak of FIr3mG3 at 77 K exhibits little increase in its intensity as compared to that of FIr3mG2, while that of FIr3mG3 at 298 K shows a dramatic increase. This result also may be due to conformational heterogeneity because intensities show different tendencies at different temperatures. However, the residual peak intensity of the donor in FIr3mG*x* is relatively small as compared to that of only the dendrimer donor without an acceptor, such as mG1 (5mCP), mG2 (mG2-OH), and mG3 (mG3-OH).[18] This indicates that S−S ET is very efficient. Obviously, T−T ET from the dendrimer donor to the acceptor plays another important role in contributing to the increase in acceptor intensity. More detailed evidence for T−T ET is shown in Figure 4b, which shows the PL spectra (excited at the donor absorption peak of 310 nm) of FIr3mG*x* at 77 K. The disappearance of the donor triplet emission spectra at around 410 nm indicates efficient T−T ET from the donor to the acceptor by the Dexter mechanism. On the basis of the DFT calculation, the distance from the Ir core to the mCP nitrogen in FIr3mG3 was 12−20 Å under the assumption that all the bonds are linked through a trans geometry. Therefore, the donor and acceptor were located within the effective Dexter energy transfer distance (<20 Å) for a good wave function overlap between the donor and the acceptor.[23] Therefore, the enhancement in the PL intensity at room temperature originates not only from S−S ET but also from T−T ET from the donor to the acceptor. In the PL spectra of the PMMA film (excited at the donor absorption peak of 310 nm), the PL intensity of the acceptor also sharply increases with the number of donors (Figure 4c). The absence of the donor peak at around 350 nm indicates a perfect energy transfer from the donor to the acceptor because of inter- and intramolecular ET. The reason for the higher ET efficiency in the film than in the solution may be because of the removal of the bottleneck phenomenon through the intermolecular ET between the donor of one dendrimer and the acceptor of a nearby dendrimer molecule as well as a less flexible film phase structure, which leads to reduced nonradiative decay.[17]

Therefore, the enhancement of the acceptor emission intensity with the number of donors and a reduction in the luminance quenching induced by bulky dendron donors will make these phosphorescent dendrimers good candidates for spin-coatable dendrimer materials in OLEDs.

Energy Transfer Efficiency. Table 3 shows the ET efficiency from the donor to the acceptor in FIr3mG*x*. The S−S and T−T ET efficiencies were measured from the steady-state PL method and the transient PL method. In the steady-state PL method, the ET efficiency was determined from the extent of the luminance quenching of the donor in the presence of the acceptor.[9,10,12,15,16] This was measured from the relative ratio between the integrated area of the singlet and triplet donor peaks in mG*x* (IA_{mGx}) and that of the residual singlet and triplet donor peaks in FIr3mG*x* ($IA_{FIr3mGx}$) at 298 and 77 K (Figure S8).[18] The ET efficiency was $(1 - IA_{FIr3mGx}/IA_{mGx}) \times 100$ (%). This method reveals that in the 2-MeTHF solution, the donor emission was almost entirely quenched in all the generations. Thus, the ET efficiency from the donor to the acceptor at 298 K was calculated to be 97, 97, and 94% for FIr3mG1, FIr3mG2, and FIr3mG3, respectively. S−S ET and T−T ET can be measured by the steady-state PL method at 77 K, if it is supposed that the singlet emission range and the triplet emission range of the donor moiety are 320−404 and 405−450 nm, respectively. At 77 K, the S−S ET efficiency was calculated to be 97, 96, and 90%, and the T−T ET efficiency was calculated to be 85, 93, and 92% for FIr3mG1, FIr3mG2, and FIr3mG3, respectively. However, this method ignores

Table 2. Lifetime of Donor Peak in FIr3mG*x* at 298 and 77 K

	τ_{360nm} (ns)[a]	τ_{360nm} (ns)[b]	τ_{411nm} (μs)[c]
FIr3mG1	<0.1	<0.1 (99%), 5.1 (1%)	0.12 (93%), 2.9 (2%)
FIr3mG2	0.19 (98%), 4.7 (2%)	0.24 (98%), 5.2 (2%)	0.24 (92%), 2.7 (8%)
FIr3mG3	0.26 (93%), 5.2 (7%)	0.65 (90%), 5.2 (10%)	0.22 (98%), 2.4 (2%)
mG1	6.6	8.2	7.0 s
mG2	7.7	7.9	6.9 s
mG3	7.2	8.1	6.9 s

[a] Lifetime of donor peak (360 nm) after excitation at 310 nm in 0.02 mM 2-MeTHF solution at 298 K. [b] Data at 77 K. [c] Lifetime of donor peak (411 nm) when excited at 310 nm in 0.02 mM 2-MeTHF solution at 77 K. The lifetime of mG*x* is measured in seconds.

Table 3. Energy Transfer Efficiency of FIr3mG*x*

	transient PL ET (%)			steady-state PL ET (%)		
	298 K	77 K		298 K	77 K	
	Φ_{360}[a]	Φ_{360}[b]	Φ_{411}[c]	Φ_s[d]	Φ_s[e]	Φ_T[f]
FIr3mG1	>99	97	>99	97	97	85
FIr3mG2	98 (96)	97 (96)	>99	97	96	93
FIr3mG3	96 (92)	94 (86)	>99	94	90	92

[a] Energy transfer (%) $= (1 - \tau_{FIr3mGx360nm}/\tau_{mGx360nm}) \times 100$ at 298 K. Data in the parentheses are ET efficiency derived from average lifetime. [b] $\tau_{FIr3mGx360nm}$ at 77 K. [c] $\tau_{FIr3mGx411nm}$ at 77 K. [d] ET efficiency was measured from relative ratio between integrated area of singlet and triplet donor peak in mG*x* (IA_{mGx}) and that of residual singlet and triplet donor peak in FIr3mG*x* ($IA_{FIr3mGx}$), $x = 1-3$. Energy transfer (%) $= (1 - IA_{FIr3mGx}/IA_{mGx}) \times 100$. [e] S−S ET efficiency at 77 K. ET was measured from relative ratio between integrated area of singlet donor peak (320−404 nm) in mG*x* (IA_{mGx}) and that of residual singlet donor peak in FIr3mG*x* ($IA_{FIr3mGx}$), $x = 1-3$. [f] T−T ET efficiency at 77 K. ET was measured from relative ratio between integrated area of triplet donor peak (405−450 nm) in mG*x* (IA_{mGx}) and that of residual triplet donor peak in FIr3mG*x* ($IA_{FIr3mGx}$), $x = 1-3$.

(15) Mugnier, J.; Pouget, J.; Bourson, J.; Valeur, B. *J. Lumin.* **1985**, *33*, 273.
(16) Bourson, J.; Mugnier, J.; Valeur, B. *Chem. Phys. Lett.* **1982**, *92*, 430.
(17) Li, B.; Xu, X.; Sun, M.; Fu, Y.; Yu, G.; Liu, Y.; Bo, Z. *Macromolecules* **2006**, *39*, 456.
(18) Detailed structures of mG*x* and measurements of energy transfer efficiency via steady-state PL method are shown in the Supporting Information.

the detection error caused by the overlap between the emission of the acceptor moiety and the triplet emission of the donor moiety above 450 nm.

The expected error in the steady-state PL method can be overcome by measuring lifetimes more precisely. The ET efficiency was measured using transient PL data (Table 3) from the following equation,[9b,10,12] assuming that the ET time constants were considerably more rapid than the unquenched luminance decay from the residual donor peak of FIr3mG*x*:[19]

$$\text{ET efficiency (\%)} = (1 - \tau_{D-A}/\tau_D) \times 100 \qquad (1)$$

where τ_{D-A} is the lifetime of the donor−acceptor conjugates (FIr3mG*x*) and τ_D is the lifetime of donors (mG*x*). The transient PL spectra for FIr3mG*x* exhibited a biexponential curve, while that of mG*x* was monoexponential at 360 and 411 nm (Figure S9).[14] The long lifetime for FIr3mG*x* (4.7−5.2 ns) at 360 nm is similar to that of mG*x*. Thus, we assume that the biexponential curve may be derived from the residual unquenched donor peak of FIr3mG*x* or from the conformational heterogeneity that prevents energy transfer. Since this donor peak contributes at most 10% or less of the total signal in all cases, its role in the overall photophysics of these molecules is relatively minor. Therefore, there is a small difference between maximum energy transfer efficiency and net energy efficiency estimated from the average lifetime of the donor peak of FIr3mG*x* (Table 2: the data in parentheses). The main components of the lifetimes of the donor moiety of FIr3mG*x* ($x = 1-3$) at 360 nm were dramatically shortened—<0.1, 0.18, and 0.26 ns for FIr3mG1, FIr3mG2, and FIr3mG3, respectively—as compared to those of mG*x*—6.6, 7.7, and 7.2 ns for mG1, mG2, and mG3, respectively—at 298 K (Table 2). The decrease in the lifetime of the donor peak in FIr3mG*x* suggests an intramolecular ET from the donor to the acceptor. The S−S ET efficiency obtained from the previously mentioned equation[9b,10] is greater than 96% in all the generations and is in good agreement with those derived from the steady-state PL method at 298 K. The lifetime of the donor peaks at 360 and 411 nm was also measured at 77 K to predict the ET efficiency more precisely. The lifetime of the donor peak at 360 nm in FIr3mG*x* was also dramatically shortened—<0.1, 0.24, and 0.65 ns for FIr3mG1, FIr3mG2, and FIr3mG3, respectively—as compared to that of mG*x*—8.2, 7.9, and 8.1 ns for mG1, mG2, and mG3, respectively—at 77 K (Table 2). The minor component for FIr3mG*x* (2.4−2.9 μs) at 411 nm may also be derived from the conformational heterogeneity. The S−S ET efficiency of FIr3mG*x* through the transient PL method at 77 K was greater than 94% for each generation, which is also in good agreement with both the transient PL method at 298 K and the steady-state PL method at 77 K. Moreover, the lifetime of FIr3mG*x* at 411 nm of the triplet donor peak was also shortened—0.12, 0.24, and 0.22 μs for FIr3mG1, FIr3mG2, and FIr3mG3, respectively—as compared to that of mG*x*—7.0, 6.9, and 6.9 s, respectively. Therefore, T−T ET via the transient PL method showed a significantly higher efficiency—greater than 99% in all generations. Both S−S and T−T ET efficiencies measured from both steady-state PL and transient PL methods show similar tendencies for each generation, which indicates that both S−S and T−T ET mechanisms are mainly involved in the increase in the acceptor emission with the generation.

(19) Doust, A. B.; Yang, X.; Dykstra, T. E.; Koo, K.; Scholes, G. D. *Appl. Phys. Lett.* **2006**, *89*, 213505.

Conclusion

In conclusion, a new phosphorescent system in which the donor and acceptor were covalently bound by a nonconjugated benzyl ether linker was developed. The solution and film PL intensities of the donor−acceptor conjugate system were greater than those of FIrpic due to efficient S−S and T−T ET from the donor to the acceptor. The S−S ET in FIr3mG*x* shows a very high efficiency of greater than 90% via the steady-state PL method and 94% via the transient PL method. Additionally, the T−T ET efficiency via the transient PL method exhibited an efficiency greater than 99%. This indicates that FIr3mG*x* exhibited good light-harvesting abilities because the mCP unit is an efficient light absorber and the core FIrpic functions as a spatial energy concentrator that drains energy from the dendrimer donor. Therefore, this system can be applied not only to emitting materials suitable for OLEDs due to the enhancement of the acceptor emission intensity but also to organic solar cells because of the good light-harvesting ability and high-energy transfer efficiency from the donor to the acceptor after changing the donor moiety to the visible light absorber.[20]

Experimental Procedures

Synthesis. ^{1}H and ^{13}C NMR spectra were recorded using an Advance 300 or 500 MHz Bruker spectrometer in chloroform-d_1, acetone-d_6, or DMSO-d_6. ^{1}H NMR chemical shifts in $CDCl_3$ were referenced to $CHCl_3$ (7.27 ppm), and ^{13}C NMR chemical shifts in $CDCl_3$ were reported relative to $CHCl_3$ (77.23 ppm). UV−vis spectra were recorded on a Beckman DU 650 spectrophotometer. Mass spectra were obtained using a MALDI-TOF MS from Bruker. High-resolution masses (HRMS) were measured by FABMS using a JEOL HP 5890 series. Lifetimes at 77 and 298 K were obtained using a FRET MASTER-1 from PTI and fluorescence spectrometer from Edinburgh, respectively. Fluorescence lifetime measurements were carried out with the EasyLife LS system using an EL295 LED and a stroboscopic detector. A low-temperature liquid nitrogen, a Dewar holder was used for the measurements at 77 K. Fluorescence spectra were recorded on a Jasco FP-7500 spectrophotometer. Analytical thin-layer chromatography was performed using Kieselgel 60_F-254 plates from Merck. Column chromatography was carried out on Merck silica gel 60 (70−230 mesh). All solvents and reagents were commercially available and used without further purification unless otherwise noted. Decomposition temperatures were obtained using a thermogravimetric analyzer (TGA) from Rheometric Scientific. Glass transition temperatures were recorded on a Jasco FP-750 spectrophotometer differential scanning calorimeter from TA Instruments.

Compounds ($C^\wedge N_2Ir(\mu\text{-}Cl)_2IrC^\wedge N_2$) were synthesized according to a modified version of the Nonoyama procedure,[21] by refluxing

(20) For the application of this system to the organic solar cell, the donor moiety should be changed to the visible light-absorber, and the absorption spectrum of the acceptor moiety should be in good overlap with the emission spectrum of the donor moiety.

(21) Nonoyama, M. *Bull. Chem. Soc. Jpn.* **1974**, *47*, 767.

$IrCl_3 \cdot nH_2O$ with 2−2.5 equiv of a cyclometalating ligand in a 3:1 mixture of 2-methoxyethanol and water for 6−7 h. The reaction mixture was cooled to room temperature, and more water was added to precipitate the product. The reaction mixture was filtered through a Büchner funnel and then washed with hexane and ethyl ether several times to provide the crude product.

Iridium(III) Bis[(4,6-difluorophenyl)-pyridinato-*N*,*C*$^{2'}$]3-hydroxypicolinate (FIrpicOH). A mixture of the crude chloro-bridged dimer (1.21 g, 1.0 mmol), 3-hydroxypicolinic acid (417 mg, 3 mmol), and sodium carbonate (2.12−3.18 g, 20−30 mmol) in 2-ethoxyethanol (70 mL) was refluxed under inert atmosphere for 4−5 h. After cooling to room temperature, the solvent was evaporated in vacuum and dissolved in methylene chloride. The organic phase was washed with water and dried over Na_2SO_4. The solvent was evaporated to give the crude product, which was applied to column chromatography on a silica gel, eluting with methylene chloride, ethyl acetate, and methyl alcohol (10:10:0.2, v/v) to provide the desired product (yield: 924 mg, 65%). ^{1}H NMR (300 MHz, DMSO-d_6): δ (ppm) 13.24 (s, 1H), 8.50 (d, 6 Hz, 1H), 8.36−8.15 (m, 2H), 8.12−8.02 (m, 2H), 7.80 (d, 6 Hz, 1H), 7.69 (d, 6 Hz, 1H), 7.53−7.49 (m, 2H), 7.37 (t, 3 Hz, 1H), 7.23 (d, 6 Hz, 1H), 6.92−6.71 (m, 2H), 5.64 (d, 3 Hz, 1H), 5.49 (d, 3 Hz, 1H). ^{13}C NMR (125 MHz, DMSO-d_6): δ (ppm) 176.93, 163.69, 163.58, 163.23, 162.85, 162.80, 161.50, 161.40, 161.21, 159.45, 159.34, 149.12, 148.11, 139.58, 139.49, 131.01, 128.24, 127.85, 124.13, 123.74, 122.89, 122.83, 122.68, 113.81, 113.67, 98.15, 97.94, 97.69. HRMS (FAB) *m*/*z*: calcd for $[C_{28}H_{16}F_4IrN_3O_3 + H]^+$ 712.0835, found $[M + H]^+$ 712.0826.

5mCP (mG1= 5-Methyl-*N*,*N*′-dicarbazolyl-1,3-benzene). This compound was prepared according to the Buchwald procedure.[22] To a mixture of CuI (780 mg, 4.1 mmol), K_3PO_4 (11.79 g, 51.25 mmol), and carbazole (6.5 g, 38.9 mmol) in toluene (100 mL) were added 1,3-dibromo-5-methylbenzene (5.0 g, 20.5 mmol) and (±)-*trans*-1,2-diaminocyclohexane (936 mg, 8.2 mmol) under nitrogen. The reaction tube was quickly sealed, and the contents were stirred while being heated in an oil bath at 110 °C for 24 h. The reaction mixture was filtered through Celite, and the solvent was evaporated in vacuo and then dissolved in methylene chloride. The organic phase was washed with water and brine and was dried with Na_2SO_4. After the solvent was evaporated, a crude product was obtained and purified by column chromatography on silica gel, eluting with methylene chloride and hexane (1:20, v/v) (yield: 6.49 g, 75%). ^{1}H NMR (300 MHz, $CDCl_3$): δ (ppm) 8.23 (d, 6 Hz, 4H), 7.70 (s, 1H), 7.66 (s, 2H), 7.62 (d, 9 Hz, 4H), 7.48 (t, 6 Hz, 4H), 7.31 (t, 6 Hz, 4H), 2.68 (s, 3H). ^{13}C NMR (125 MHz, acetone-d_6): δ (ppm) 143.29, 141.70, 140.03, 127.63, 127.19, 124.47, 123.24, 121.29, 121.20, 110.82, 105.58. MALDI-TOF: calcd for $C_{31}H_{22}N_2$ 422.18, found 422.25. HRMS (FAB): calcd for $C_{31}H_{22}N_2$ 422.1782, found 422.1783.

5mCP-Br (mG1-Br = 5-Bromomethyl-*N*,*N*′-dicarbazolyl-1,3-benzene). A mixture of 5mCP (7.0 g, 16.5 mmol), 0.8−0.9 equiv of NBS (1.13 g, 19.8 mmol), and benzoyl peroxide (400 mg, 1.65 mmol) in CCl_4 (150 mL) was heated at reflux temperature for 10 h. After the reaction was complete, the reaction mixture was filtered through a Büchner funnel and then washed with CCl_4. The solvent was evaporated in vacuum. The resulting mixture was dissolved in methylene chloride and washed with water and dried over Na_2SO_4. The solvent was evaporated to give the crude product, which was applied to column chromatography on silica gel, eluting with hexane to provide the desired product (yield: 4.62 g, 56%). ^{1}H NMR (300 MHz, $CDCl_3$): δ (ppm) 8.25 (d, 9 Hz, 4H), 7.89 (s, 2H), 7.81 (s, 1H), 7.46 (d, 9 Hz, 4H), 7.30 (t, 6 Hz, 4H), 7.17 (t, 6 Hz, 4H), 5.00 (s, 2H). ^{13}C NMR (125 MHz, $CDCl_3$): δ (ppm) 141.70, 140.59, 139.85, 126.47, 125.88, 124.97, 123.91, 120.95, 120.77, 110.05, 39.19. MALDI-TOF: calcd for $C_{31}H_{21}BrN_2$ 500.09, found 500.06. Anal. calcd for $C_{31}H_{21}BrN_2 \cdot H_2O$: C 71.68; H 4.46; N 5.39. Found: C 71.26; H 4.14; N 5.76.

mG2-OH (mG2). To a solution of 3,5-dihydroxybenzyl alcohol (280 mg, 2.0 mmol) in acetone (120 mL) were added 5mCP-Br (2.0 g, 4.0 mmol), K_2CO_3 (1.38 g, 10 mmol), and 18-crown-6 (52 mg, 0.2 mmol). The reaction mixture was refluxed for 8 h. After cooling to room temperature, the solvent was evaporated in vacuum and dissolved in methylene chloride. The organic phase was washed with water and dried over Na_2SO_4. The solvent was evaporated to give the crude product, which was applied to column chromatography on silica gel, eluting with methylene chloride and hexane (1:10, v/v) to provide the desired product (yield: 1.67 g, 85%). ^{1}H NMR (300 MHz, $CDCl_3$): δ (ppm) 8.12 (d, 6 Hz, 8H), 7.75 (s, 4H), 7.70 (s, 2H), 7.50 (d, 9 Hz, 8H), 7.40 (t, 15 Hz, 8H), 7.26 (t, 12 Hz, 8H), 6.81 (s, 2H), 6.74 (s, 1H), 5.31 (s, 4H), 4.70 (s, 2H), 3.49 (s, 1H). ^{13}C NMR (125 MHz, $CDCl_3$): δ (ppm) 159.92, 144.17, 141.02, 140.68, 139.81, 126.39, 124.60, 124.43, 123.86, 120.67, 120.63, 109.87, 106.45, 101.94, 69.33, 65.31. MALDI-TOF: calcd for $C_{69}H_{48}N_4O_3$ 980.37, found 980.32. Anal. calcd for $C_{69}H_{48}N_4O_3 \cdot H_2O$: C 82.94; H 5.04; N 5.61. Found: C 82.93; H 5.27; N 5.34.

mG2-Br. A mixture of mG2-OH (1.8 g, 1.83 mmol) and PBr_3 (593 mg, 2.2 mmol) in methylene chloride (100 mL) was stirred at 0 °C for 2 h. After completing the reaction, methanol was added to quench the residual PBr_3. (*Caution: this will produce the volatile methyl bromide.*) All volatiles were evaporated in vacuum and dissolved in methylene chloride. The organic phase was washed with water and dried over Na_2SO_4. The solvent was evaporated to give the crude product, which was applied to column chromatography on silica gel, eluting with methylene chloride and hexane (1:20, v/v) to provide the desired product (yield: 1.68 g, 92%). ^{1}H NMR (300 MHz, $CDCl_3$): δ (ppm) 8.20 (d, 9 Hz, 8H), 7.90 (s, 4H), 7.83 (s, 2H), 7.56 (d, 9 Hz, 8H), 7.39 (t, 9 Hz, 8H), 7.26 (t, 15 Hz, 8H), 6.94 (s, 2H), 6.90 (s, 1H), 5.55 (s, 4H), 4.62 (s, 2H).^{13}C NMR (125 MHz, $CDCl_3$): δ (ppm) 159.82, 140.86, 69.40, 33.38. MALDI-TOF: calcd for $[M + H]^+$ 1043.29, found 1043.42. Anal. calcd for $C_{69}H_{47}BrN_4O_2 \cdot H_2O$: C 78.03; H 4.65; N 5.28. Found: C 78.16; H 5.03; N 4.93.

mG3-OH (mG3). To a solution of 3,5-dihydroxybenzyl alcohol (87.5 mg, 0.625 mmol) in acetone (70 mL) were added mG2-Br (1.3 g, 1.25 mmol), K_2CO_3 (432 mg, 3.13 mmol), and 18-crown-6 (16.5 mg, 0.0625 mmol). The reaction mixture was refluxed for 8 h. After cooling to room temperature, the solvent was evaporated in vacuum and dissolved in methylene chloride. The organic phase was washed with water and dried over Na_2SO_4. The solvent was evaporated to give the crude product, which was applied to column chromatography on silica gel, eluting with methylene chloride and hexane (1:10, v/v) to provide the desired product (yield: 1.00 g, 78%). ^{1}H NMR (300 MHz, $CDCl_3$): δ (ppm) 8.10 (d, 9 Hz, 16H), 7.74 (s, 8H), 7.72(s, 4H), 7.50 (d, 9 Hz, 16H), 7.37 (t, 15 Hz, 16H), 7.24 (t, 15 Hz, 16H), 6.75 (s, 4H), 6.65 (s, 2H), 6.54 (s, 2H), 6.48 (s, 1H), 5.31 (s, 8H), 4.94 (s, 4H) 4.56 (s, 2H).^{13}C NMR (125 MHz, $CDCl_3$): δ (ppm) 160.15, 159.86, 143.72, 140.92, 140.65, 140.03, 139.79, 139.31, 126.38, 124.58, 124.39, 123.83, 120.65, 120.61, 109.85, 107.03, 105.97, 102.23, 101.45, 69.32, 65.29. MALDI-TOF: calcd for $[M + H]^+$ 2065.77, found 2065.11. Anal. calcd for $C_{145}H_{100}N_8O_7 \cdot H_2O$: C 83.55; H 4.93; N 5.38. Found: C 82.65; H 4.87; N 5.29.

(22) Antilla, J. C.; Klapars, A.; Buchwald, S. L. *J. Am. Chem. Soc.* **2002**, *124*, 11684.
(23) Shoustikov, A. A.; You, Y.; Thompson, M. E. *IEEE J. Sel. Top. Quantum Electron.* **1998**, *4*, 3.

mG3-Br. A mixture of G3-OH (600 mg, 0.29 mmol) and PBr_3 (157 mg, 0.58 mmol) in methylene chloride (50 mL) was stirred at 0 °C for 10 h. After completing the reaction, methanol was added to quench the residual PBr_3. (*Caution: this will produce the volatile methyl bromide*.) All volatiles were evaporated in vacuum and dissolved in methylene chloride. The organic phase was washed with water and dried over Na_2SO_4. The solvent was evaporated to give the crude product, which was applied to column chromatography on silica gel, eluting with methylene chloride and hexane (1:20, v/v) to provide the desired product (yield: 460 mg, 75%). ^{1}H NMR (300 MHz, $CDCl_3$): δ (ppm) 8.11 (d, 9 Hz, 16H), 7.74 (s, 8H), 7.73 (s, 4H), 7.49 (d, 9 Hz, 16H), 7.38 (t, 9 Hz, 16H), 7.26 (t, 15 Hz, 16H), 6.73 (s, 4H), 6.67 (s, 2H), 6.59 (s, 2H), 6.58 (s, 1H), 5.26 (s, 8H), 4.94 (s, 4H) 4.27 (s, 2H). ^{13}C NMR (125 MHz, $CDCl_3$): δ (ppm) 160.05, 159.87, 140.90, 140.65, 140.09, 139.80, 139.76, 126.38, 124.58, 124.39, 123.84, 120.65, 120.62, 109.84, 108.45, 107.09, 102.38, 102.30, 70.02, 69.33, 33.62. MALDI-TOF: calcd for $C_{145}H_{99}BrN_8O_6$ 2126.69, found 2126.67. Anal. calcd for $C_{145}H_{99}BrN_8O_6 \cdot H_2O$: C 81.10; H 4.74; N 5.22. Found: C 80.59; H 4.85; N 5.11.

FIr3mG1. To a solution of FIrpicOH (1.00 g, 1.36 mmol) in acetone (100 mL) were added 5mCP-Br (682 mg, 1.36 mmol) and Cs_2CO_3 (489 mg, 1.5 mmol). The reaction mixture was refluxed for 7 h. After cooling to room temperature, the solvent was evaporated in vacuum and dissolved in methylene chloride. The organic phase was washed with water and dried over Na_2SO_4. The solvent was evaporated to give the crude product, which was applied to column chromatography on silica gel, eluting with methylene chloride, ethyl acetate, and methyl alcohol (10:10:0.2, v/v) to provide the product. To remove any residual impurity, trituration was carried out in CH_2Cl_2 and hexane (1:20, v/v). The solidified product was filtered through a Büchner funnel and then washed with hexane and ethyl ether several times to provide the desired product. (yield: 1.24 g, 81%). ^{1}H NMR (300 MHz, acetone-d_6): δ (ppm) 8.70 (d, 5.4 Hz, 1H) 8.40 (d, 1.2 Hz, 1H) 8.31 (s, 1H) 8.28−8.21 (m, 4H) 8.06 (t, 6 Hz, 3H) 7.96−7.88 (m, 3H) 7.78 (d, 6 Hz, 1H), 7.66−7.60 (m, 6H), 7.57 (s, 1H), 7.49−7.42 (m, 4H), 7.35−7.27 (m, 4H), 7.12−7.12 (m, 1H), 6.66−6.50 (m, 2H), 5.83 (d. 9 Hz, 1H), 5.59 (s, 2H), 5.55 (d, 8.1 Hz, 1H). ^{13}C NMR (125 MHz, DMSO-d_6): 169.93, 163.61, 163.03, 162.94, 157.83, 148.86, 147.93, 140.24, 139.83, 139.27, 138.65, 138.06, 128.73, 127.23, 126.41, 124.94, 124.24, 123.11, 122.95, 121.90, 121.10, 120.52, 112.40, 111.95, 110.12, 109.89, 97.64, 69.34. HRMS (FAB): calcd for $[M + H]^+$ 1132.2461, found 1132.2455. Anal. calcd for $C_{59}H_{36}F_4IrN_5O_3 \cdot H_2O$: C 61.66; H 3.33; N 6.09. Found: C 61.33; H 3.20; N 6.13.

FIr3mG2. To a solution of FIrpicOH (618 mg, 0.843 mmol) in DMF (20 mL) were added mG2-Br (800 mg, 0.766 mmol) and Cs_2CO_3 (411 mg, 1.26 mmol). The reaction mixture was refluxed for 7 h. After cooling to room temperature, the solvent was evaporated in vacuum and dissolved in methylene chloride. The organic phase was washed with water and dried over Na_2SO_4. The solvent was evaporated to give the crude product, which was applied to column chromatography on silica gel, eluting with methylene chloride, ethyl acetate, and methyl alcohol (10:10:0.2, v/v) to provide the product. To remove any residual impurity, trituration was carried out in CH_2Cl_2 and hexane (1:20, v/v). The solidified product was filtered through a Büchner funnel and then washed with hexane and ethyl ether several times to provide the desired product (yield: 1.01 g, 72%). ^{1}H NMR (300 MHz, acetone-d_6): δ (ppm) 8.69 (d, 6.9 Hz 1H), 8.27 (d, 8.4 Hz, 2H), 8.18 (d, 8.4 Hz, 8H), 7.93−7.83 (m, 6H), 7.76−7.72 (m, 4H), 7.58 (d, 4.5 Hz 8H), 7.58−7.57 (m, 2H), 7.49−7.31 (m, 10H), 7.24−7.19 (m, 8H), 6.83 (s, 3H), 6.64−6.51 (m, 2H), 5.81 (d, 9.6 Hz 1H), 5.62−5.55 (m, 5H), 5.38 (s, 2H). ^{13}C NMR (125 MHz, DMSO-d_6): 177.06, 170.11, 159.82, 159.25, 157.89, 149.19, 148.14, 141,44, 140.20, 139.82, 139.65, 139.57, 139.27, 138.49, 138,37, 132.94, 131.46, 127.57, 126.32, 124.18, 123.31, 122.91, 120.46, 120.26, 113.83, 113.69, 109.69, 106.07, 101.85, 97.83, 69.65, 68.18. HRMS (FAB): calcd for $[C_{97}H_{62}F_4IrN_7O_5 + H]^+$ 1674.4456, found 1674.4462.

FIr3mG3. To a solution of FIrpicOH (210 mg, 0.282 mmol) in DMF (10 mL) were added mG3-Br (600 mg, 0.282 mmol) and Cs_2CO_3 (138 mg, 0.423 mmol). The reaction mixture was refluxed for 7 h. After cooling to room temperature, the solvent was evaporated in high vacuum and dissolved in methylene chloride. The organic phase was washed with water and dried over Na_2SO_4. The solvent was evaporated to give the crude product, which was applied to column chromatography on silica gel, eluting with methylene chloride, ethyl acetate, and methyl alcohol (10:10:1, v/v) to provide the desired product. To remove any residual impurity, trituration was carried out in CH_2Cl_2 and hexane (1:20, v/v). The solidified product was filtered through a Büchner funnel and then washed with hexane and ethyl ether several times to provide the desired product. (yield: 230 mg, 30%). ^{1}H NMR (300 MHz, DMSO-d_6): δ (ppm) 8.54 (d, 4.8 Hz 1H), 8.18−8.13 (m, 18H), 7.97−7.84 (m, 2H), 7.77−7.70 (m, 13H), 7.65−7.61 (m, 2H), 7.47−7.44 (m, 18H), 7.35−7.26 (m, 18H), 7.18 (t, 4.5 Hz, 16H), 6.87 (m, 8H), 6.66−6.47 (m, 2H), 5.63 (d, 8.1 Hz, 1H), 5.47−5.35 (m, 9H), 5.50 (s, 2H), 4.96 (s, 4H). ^{13}C NMR (125 MHz, DMSO-d_6): 170.10, 163.65, 162.97, 161.64, 161.21, 159.40, 159.13, 157.80, 154.27, 153.46, 148.75, 147.91, 141.38, 139.77, 139.55, 139.14, 138.73, 138.44, 138.28, 127.92, 127.83, 126.22, 124.08, 123.72, 123.21, 122.88, 120.79, 120.39, 120.22, 113.69, 109.59, 107.15, 105.40, 102.07, 101.14, 69.49, 69.15, 68.18. MALDI-TOF: calcd for $C_{173}H_{114}F_4IrN_{11}O_9$ 2757.84, found 2757.74. Anal. calcd for $C_{173}H_{114}F_4IrN_{11}O_9$: C 75.31; H 4.16; N 5.58. Found: C 75.12; H 4.41; N 5.40.

Acknowledgment. We thank Samsung SDI−SNU for a grant and the Seoul R&D Program for financial support. We also acknowledge the BK 21 fellowship grants to T.-H.K. and J.K. C.-L.L. thanks the Cambridge-KAIST Collaboration Program for financial support. Transient PL data was provided by Dr. Alex Siemiarczuk of PTI.

Supporting Information Available: DFT calculations; TGA, DSC, UV, and PL data of dendrimer donor mG*x*; measurement of energy transfer efficiency via steady-state PL method; and transient PL data. This material is available free of charge via the Internet at http://pubs.acs.org.

CM070536K